Eliassen, A., Høiland E. and Riis, E., " Two-dimensional perturbation of a flow with constant shear of stratified fluid, " *Inst. for Wea. and Climate Res. or Inst. of Theor. Astrophys.*, Oslo, Publibation No. 1 (1953).
Kato, T., *Perturbation Theory for Linear Operators*, Springer-Verlag New York Inc., 592 pp. (1966).
Lin., C. C., *The Theory of Hydrodynamic Stability.* London and New York, Cambridge Univ. Press., 122–123 (1966).
McIntyre, M. E., " A separable nongeostrophic baroclinic stability problem, " *J. Atmos. Sci.* **22**, 730–731 (1965).
McIntyre, M. E., " On the non-separable baroclinic parallel-flow instability problem." *J. Fluid Mech.* (1969) (In press).
Morse, P. M. and Feshbach, H., *Methods of Theoretical Physics, Vol. II*, New York, McGraw-Hill Book Company, Inc., 999–1106 (1953).
Orr, W. McF., " The stability or instability of the steady motions of a perfect liquid and of a viscous liquid, " *Proc. Roy. Irish Acad.* **27**, 9–138 (1907).
Pedlosky, J., " An initial value problem in the theory of baroclinic instability, " *Tellus* **16**, 12–17 (1964).
Phillips, N. A., " An overlooked aspect of the baroclinic stability problem, " *Tellus* **16**, 268–270 (1964).
Rellich, F., *Perturbation Theory on Eigenvalue Problems.* Notes, New York Univ. Available from University Microfilm, Ann Arbor, Michigan (1953). (To be published by Gordon and Breach, Co.)
Sela, J., " On baroclinic and barotropic ageostrophic stability." Ph. D. Thesis, Univ. of Michigan. Also available as technical report 07344–2–T, Dept. of Meteor. and Ocean., Univ. of Michigan, Ann Arbor, 98 pp. (1968).
Stone, P. H., " On non-geostrophic baroclinic stability, " *J. Atmos. Sci.* **23**, 390–400 (1966).
Tareyev, B. A., " Non-geostrophic disturbances and baroclinic instability in two-layered oceanic flow." *Izvestiya*, Atmospheric and Oceanic Physics, 4, 730–734 in English edition or 1275–1284 in Russian edition (1968).

Geophysical Fluid Dynamics. 1970. Vol. 1, pp. 123–142

Printed in Great Britain

Self-Convection of Floating Heat Sources: A Model for Continental Drift

L. N. HOWARD and W. V. R. MALKUS
Department of Mathematics, M.I.T.
and
J. A. WHITEHEAD
Institute of Geophysics and Planetary Physics, U.C.L.A.

Abstract—Two models of floating heat sources are studied. In the first model the motion of two line heat sources constrained to float at an arbitrary depth in a viscous fluid is determined in the limit of small convection velocities. It is found that the sources drift apart and at great separation attain a constant velocity proportional to the square root of the heat flux. The second model is a floating block heat source, presumed to be very long compared to its depth. It is found to exhibit periodic excursions between the end walls of the fluid container with the same dependence of velocity on heat flux as the line sources. A series of experiments are described which exhibit various features of the theory. The numerical values found when the theory is applied to the earth suggest that the idealized flows may be useful in the interpretation of continental drift.

Introduction

Geophysical literature of the past few years has been filled with fascinating observations on the drift of continents. The new global tectonics (Isacks *et al.*, 1968) paints a picture of North and South America moving away from Africa and Europe at a rate of approximately four centimeters a year with significant upwelling of deep material in the mid-Atlantic ridge. This motion has forced the crust of the Pacific Ocean to turn down at the continental edges, producing the ring of earthquakes and vulcanism in the Pacific basin. The exploration of this global convection adds new understanding of the history of our earth every month. However, the dynamical basis for this motion has been investigated in only a casual fashion. The story told in the literature is of convective motions due to heat sources deep in the mantle of the earth, moving the (passive) continents around; yet there is no evidence for an energy source at depth to provide for such convective processes.

The only well-established source of heat is the uranium and other radioactive materials in the continental masses themselves and a smaller amount in the oceanic basalt. A source of heating in the continental material on top of deeper, perhaps less viscous material, would be a stabilizing effect in the usual convective sense. However, as early as 1935 Pekeris established that convection would exist due to an imposed horizontal temperature gradient, even though the underlying fluid were stable. Pekeris did not discuss, nor at that time was it determined that continents were drifting, but he did suggest that temperature differences of 100 degrees or so between continental structures and oceanic structures would lead to fluid motions of about a centimeter a year. Pekeris assumed certain smooth global distributions of temperature variation and computed the slow velocity fields which would result from these temperature distributions in a uniform fluid.

In this work we will explore the consequences of the assumption that the principal source of heat for continental motion is the distribution of radioactive materials in the continental and oceanic crust. Our models are attempts to isolate the simplest examples of motion induced by such horizontal inhomogeneity in heating and yet retain what we believe to be those features most essential for models which may have usefulness in the general interpretation of geophysical data. While we consequently have excluded the variation of viscosity with depth, the solidification of crustal material, and of course the geometric complexity of the real geophysical process, we can yet hope that if the significant dynamical aspects of the continental drifting phenomenon are contained in our idealization some of these complexities can be added at a later date.

1. Drifting Line Heat Sources

Both models we construct are approximately realizable in the laboratory, with the purpose in mind of testing the limits of validity of our theoretical proposals. This first model has the virtue that theoretical results for the entire field of motion can be attained. It has the disadvantage of mathematical complexity and un-geophysical appearance. We encourage the earth-scientist first to read section 2, returning to this section with such doubts as are raised in his mind there.

We consider two line heat sources of strength Q per unit length in a fluid of depth h. The heat sources are constrained to move at a depth d and at any instant are a distance $2a$ apart. The upper and lower bounding surfaces are isothermal, the lower one being held at a temperature ΔT above that of the upper. We consider two dimensional motions induced by these heat sources, the stream function for such motion satisfying the condition that it and its second derivative with respect to the vertical coordinate (z) vanish at the upper and lower surface, i.e. rigid slippery boundaries. On the line of symmetry between these two sources, the stream function and its second derivative with respect to the horizontal coordinate (x) vanish and the horizontal gradient of the temperature also vanishes. Figure 1 indicates one-half of this symmetric distribution.

As posed, this problem is well-suited for numerical computation even when the viscosity is a complicated function of temperature. However, we seek analytical solutions and prescribe the kinematic viscosity (ν), the thermometric conductivity (κ), and the coefficient of expansion (α) of the fluid to be everywhere the same. The Boussinesq descriptions of the dynamics and thermodynamics of this fluid are given in Eqs. (1.1) and (1.2)

$$\frac{D\omega}{Dt} + \alpha g T_x = \nu \nabla^2 \omega \tag{1.1}$$

$$\frac{DT}{Dt} + \beta \psi_x = \kappa \nabla^2 T + Q\delta(x-a)\delta(z+d) \tag{1.2}$$

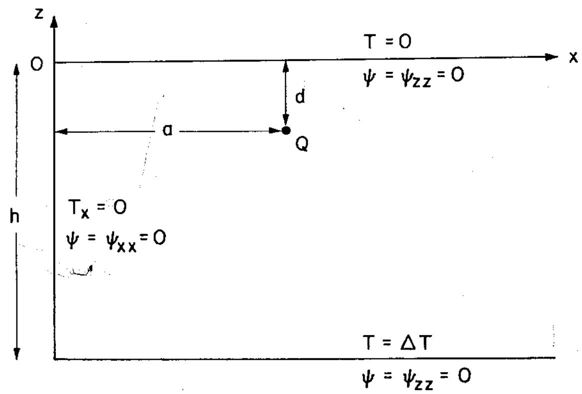

Figure 1. Geometry and boundary conditions for the drifting line heat source, Q.

where $\beta = -\Delta T/h$, D/Dt is the substantial derivative, subscripts indicate partial differentiation, and δ is the Dirac delta function. Here we require that ΔT always be less than the critical temperature difference needed to initiate free cellular convection. The relations of the stream function (ψ) to the vorticity (ω), to the horizontal velocity (u), and to the vertical velocity (w) are

$$\nabla^2\psi = \omega, \qquad \psi_z = u, \qquad -\psi_x = w \tag{1.3}$$

The problem is completed by Eq. (1.4), which is the essential statement that the time derivative of source position is equal to the horizontal velocity in the fluid at the position of the source.

$$a_t = \psi_z(a, -d) \equiv U \tag{1.4}$$

A scaling of the variables of this problem, based on the linear response (V) for fixed a and $\beta = 0$, is

$$\psi = (Vh)\psi', \qquad r = (h)r', \qquad T = \left(\frac{Q}{\kappa}\right)T'$$

$$\delta = (h^{-1})\delta', \qquad t = \left(\frac{h^2}{\kappa}\right)t', \qquad V \equiv \left(\frac{\alpha g Q h^2}{\kappa\nu}\right) \tag{1.5}$$

We now drop the primes in this scaling and rephrase the physics

of our problem as

$$\frac{1}{\sigma}\{\nabla^2\psi_t + \mathrm{R}\,(\mathbf{v}\cdot\nabla)\nabla^2\psi\} + T_x = \nabla^4\psi \tag{1.6}$$

$$T_t + \mathrm{R}\,\mathbf{v}\cdot\nabla T + \mathrm{R_a}\,\psi_x = \nabla^2 T + \delta(x-a)\delta(z+d) \tag{1.7}$$

$$U = \mathrm{R}\,\psi_z(a, -d) \tag{1.8}$$

$$\sigma \equiv \frac{\nu}{\kappa}, \qquad \mathrm{R_a} = \frac{\alpha g\beta h^4}{\kappa\nu}, \qquad \mathrm{R} = \frac{Vh}{\kappa} = \frac{\alpha g Q h^3}{\nu\kappa^2} \tag{1.9}$$

in terms of the three independent physical parameters; the Prandtl number σ, the Rayleigh number $\mathrm{R_a}$, and a thermal Reynolds number R.

It is relevant to the drifting continent problem to seek solutions of Eqs. (1.6, 7, 8) for $1/\sigma$ vanishingly small. However, we would like to know the field of motion for R both small and large. An expansion of ψ and T in a power series in R can give us valid solutions for small R and some insight, perhaps, into the character of the solutions at larger R. The leading equations in an R expansion, for vanishingly small $1/\sigma$, are

$$T_x = \nabla^4\psi \tag{1.10}$$

$$T_t + \mathrm{R_a}\,\psi_x = \nabla^2 T + \delta(x-a)\delta(z+d) \tag{1.11}$$

The next higher order equations in R are the linear inhomogeneous set

$$T_{1x} = \nabla^4\psi_1 \tag{1.12}$$

$$T_{1t} + \mathrm{R_a}\,\psi_{1x} - \nabla^2 T_1 = -\mathbf{v}\cdot\nabla T \tag{1.13}$$

whose solution depends on the solutions found for Eqs. (1.10, 11).

To solve Eqs. (1.10, 11), one first constructs the Fourier transforms appropriate to our boundary conditions,

$$\theta(k, m) = \int_0^\infty \cos kx\,dx \int_{-1}^0 T(x, z)\sin m\pi z\,dz$$

$$\phi(k, m) = \int_0^\infty \sin kx\,dx \int_{-1}^0 \psi(x, z)\sin m\pi z\,dz \tag{1.14}$$

hence

$$T(x, z) = \frac{4}{\pi}\int_0^\infty \cos kx \, dk \sum_{m=1}^{\infty} -\theta(k, m) \sin m\pi(-z)$$

$$\psi(x, z) = \frac{4}{\pi}\int_0^\infty \sin kx \, dk \sum_{m=1}^{\infty} -\phi(k, m) \sin m\pi(-z) \quad (1.15)$$

Then, from Eqs. (1.10, 11), the equations satisfied by θ and ϕ are

$$-k\theta = (k^2+\pi^2m^2)^2\phi \quad (1.16)$$

$$\theta_t + k\,\mathrm{R_a}\,\phi + (k^2+\pi^2m^2)\theta = -\cos ka \sin m\pi d \quad (1.17)$$

The solution of Eqs. (1.16, 17) for θ is, with $\theta = 0$ initially:

$$\theta = -\sin m\pi d \, e^{-[\ ]t}\int_0^t e^{+[\ ]\tau} \cos ka(\tau)\, d\tau \quad (1.18)$$

where

$$[\ ] = \left((k^2+\pi^2m^2) - \frac{\mathrm{R_a}\,k^2}{(k^2+\pi^2m^2)^2}\right) \quad (1.19)$$

Hence, from Eqs. (1.15, 16),

$$\psi_z(a, -d) = \sum_{m=1}^{\infty} m \sin(2\pi d)m \int_0^\infty \frac{k\,dk}{(k^2+\pi^2m^2)^2}\int_0^t e^{-[\ ]\eta}\{\ \}\, d\eta,$$

$$\eta \equiv t-\tau, \ \{\ \} \equiv \{\sin k[a(t)+a(\tau)] + \sin k[a(t)-a(\tau)]\} \quad (1.20)$$

With Eq. (1.4), Eq. (1.20) constitutes a formal solution to the first-order problem. However, Eq. (1.20) also contains higher-order features of the flow because $a(t)$ has not been linearized. It is instructive to include the first advective effects of the source by considering the expansion

$$a(\tau) = a(t) - a_t\,\eta + \tfrac{1}{2}a_{tt}\,\eta^2 + \cdots \quad (1.21)$$

Then the retention of both $a(t)$ and $a_t\,\eta$ terms in Eq. (1.21) for use in Eq. (1.20) corresponds to the inclusion of both first and second-order R terms for the source. Alternatively, one can restate the problem as that of determining the R which will produce a linear flow at the source equal to an imposed constant source velocity U.

With the neglect of $a_{tt}\,\eta^2$ and higher terms in Eq. (1.21), one can explicitly evaluate the time integral in Eq. (1.20) as

$$\int_0^t e^{-[\ ]\eta}\{\ \}\, d\eta = F \sin 2ak + G(1-\cos 2ak),$$

$$F = \frac{\{-[\ ]\cos kUt + kU \sin kUt\}\, e^{-[\ ]t} + [\ ]}{[\ ]^2 + k^2U^2} \quad (1.22)$$

$$G = \frac{\{-[\ ]\sin kUt - kU \cos kUt\}\, e^{-[\ ]t} + kU}{[\ ]^2 + k^2U^2}$$

For a certain time after the source Q is first turned on the time dependent terms in Eq. (1.22) will be important. However, for

$$t \gg \frac{1}{[\ ]_{\text{minimum}}} \equiv t_c \quad (1.23)$$

the time-dependence vanishes and

$$\int_0^{t \gg t_c} e^{-[\ ]\eta}\{\ \}\, d\eta = \frac{[\ ]\sin 2ak + kU(1-\cos 2ak)}{[\ ]^2 + k^2U^2} \quad (1.24)$$

Hence, the k integral in Eq. (1.21) may be written

$$\int_0^\infty \frac{k\,dk}{(k^2+\pi^2m^2)^2}\int_0^{t \gg t_c} e^{-[\ ]\eta}\{\ \}\, d\eta =$$

$$\frac{i}{2}\int_{-\infty}^{+\infty} \frac{k(1-e^{i2ak})\, dk}{\{(k^2+\pi^2m^2)^3 - k^2\,\mathrm{R_a} + ikU(k^2+\pi^2m^2)^2\}} \quad (1.25)$$

simplifying the form of Eq. (1.24) by the use of complex notation. Then utilizing Eqs. (1.4) and (1.20, 25), one concludes that

$$U = \frac{\mathrm{R}}{2\pi^4}\sum_{m=1}^{\infty} \frac{\sin(2\pi d)m}{m^3}\int_{-\infty}^{+\infty} \frac{ik(1-e^{ibk})\, dk}{(k^2+1)^3 - \gamma k^2 + ikv(k^2+1)^2} \quad (1.26)$$

where $\quad b \equiv (2\pi a)m, \quad \gamma \equiv \mathrm{R_a}/\pi^4m^4, \quad v \equiv U/\pi m.$

The problem remaining is to evaluate the k integral and the m sum as a function of γ, i.e. the Rayleigh number. This can be done readily for $\mathrm{R_a} = 0$ and for $\mathrm{R_a}$ close to its critical value for free convection. Intermediate values for $\mathrm{R_a}$ involve the determination of the complex roots of the sextic equation

$$(k^2+1)^3-\gamma k^2+ikv(k^2+1)^2=0 \tag{1.27}$$

For $\gamma=0$, the roots of Eq. (1.27) are

$$k=\pm\ i,\ \pm i,\ \frac{i}{2}(-v\pm\sqrt{v^2+4}) \tag{1.28}$$

Therefore

$$U=\left(\frac{\mathrm{R}}{4\pi^3}\right)\sum_{m=1}^{\infty}\frac{\sin(2\pi d)m}{m^3}\left(\frac{v}{\sqrt{v^2+4}(2+\sqrt{v^2+4})}+H\mathrm{e}^{-b}\right)$$

$$\text{where}\quad H\equiv\frac{2+(1+b)v}{v^2}-\frac{8\,\mathrm{e}^{+b(1-(\sqrt{v^2+4}-v)/2)}}{v^2\sqrt{v^2+4}(\sqrt{v^2+4}-v)} \tag{1.29}$$

$$\simeq\tfrac{1}{4}b(1+b),\qquad\text{for}\qquad v\ll 1.$$

It is seen that the m series converges with great rapidity in most cases. For $d=\frac{1}{4}$, roughly 0.98 of U is contained in the first term, $m=1$. Also from Eq. (1.29), it is clear that the velocity of the initial separation of the two heat sources is proportional to R, dropping off exponentially with increasing separation. At distances large compared to $h/2\pi$, for $d=\frac{1}{4}$ and $m=1$,

$$U^2=\pi^2(\sqrt{(\mathrm{R}/4\pi^4)+1}+1)(\sqrt{(\mathrm{R}/4\pi^4)+1}-3) \tag{1.30}$$

Hence

$$U\simeq\frac{1}{\sqrt{6}\pi}\sqrt{\mathrm{R}-\mathrm{R}_c},\qquad \mathrm{R}_c\equiv 32\pi^4 \tag{1.31}$$

for $\qquad \mathrm{R}\geqslant\mathrm{R}_c$

and

$$U\simeq\frac{1}{2\pi}\sqrt{\mathrm{R}-\mathrm{R}_c},\qquad \mathrm{R}\gg\mathrm{R}_c. \tag{1.32}$$

This latter conclusion, Eq. (1.30), is entirely the consequence of retaining the second-order motion term, Eq. (1.21). Hence the square-root dependence of U on R at great separation distance must be considered suspect until the remaining second-order terms in the flow field ψ are determined.

The second case for which the k integral can be determined without great labor is for

$$\gamma=\tfrac{27}{4}-\varepsilon \tag{1.33}$$

where both ε and v will be considered to be much smaller than one. We again choose $d=\frac{1}{4}$ and find that the $m=1$ contribution to the flow is

$$U\simeq\left(\frac{\mathrm{R}}{2\pi^2}\right)\frac{2\sqrt{2}}{9}\frac{\pi}{p^2+q^2}\left\{q+\left(q\cos\left(\frac{1+v}{\sqrt{2}}\right)b-p\sin\left(\frac{1+v}{\sqrt{2}}\right)b\right)\times\mathrm{e}^{-b\varepsilon/q}\right\}$$

where

$$\sqrt{\frac{2\varepsilon}{9}+i\frac{v}{\sqrt{2}}}=p+iq \tag{1.34}$$

As in the $\gamma=0$ case, one finds that U has an initial exponential decay, but here the decay is reduced by $\varepsilon/9$ and the velocity oscillates with a spatial period reflecting the free convection cells which would occur if $\varepsilon<0$. At great separation distance, two different limiting velocities result from Eq. (1.34). For an ε chosen so that it is much smaller than v.

$$U=2\sqrt{2}\pi\left(\frac{\mathrm{R}}{36\pi^4}\right)^{2/3} \tag{1.35}$$

This result involves two limiting processes ($\varepsilon\to 0$ and $\mathrm{R}\to 0$) and suggests that one must reconsider the neglected time terms in Eq. (1.22), for as $\varepsilon\to 0$, $t_c\to\infty$. However, for $\varepsilon\gg v$, one finds from Eq. (1.34) that

$$U=\frac{12\pi}{\sqrt{5}\sqrt{\varepsilon}}\sqrt{\left(\frac{\mathrm{R}}{36\pi^4}\right)^2-\tfrac{1}{4}(\tfrac{2}{9}\varepsilon)^3} \tag{1.36}$$

These conclusions, Eqs. (1.35, 36), indicate the significant increase in U at a given R which may occur as the stability of the fluid is decreased. However, these results are restricted to small values of U. A computation of Eq. (1.26) for small ε but large U indicates that U varies as the square root of R as in the $\gamma=0$ case.

2. Drifting Block Heat Source

This second, more geophysically oriented, model is pictured in Fig. 2. A two-dimensional block of width L is immersed to a

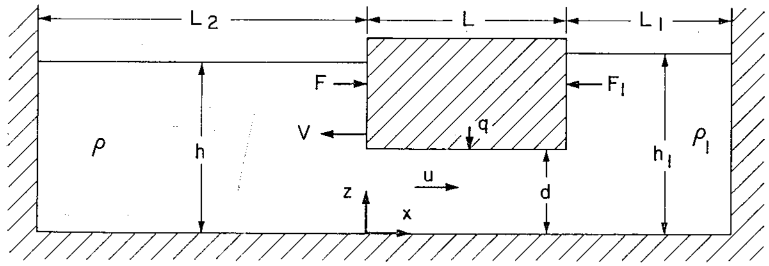

Figure 2. Block heat source drifting to left due to heat flux q into " channel " d.

depth $(h-d)$ in a fluid of depth h. The block is a heat source of strength q per unit length on its lower face. The fluid is contained in a region L_1+L_2+L long with insulating side and bottom walls. To achieve a thermodynamically steady-state model we presume that the fluid is a uniform heat sink whose strength is sufficient to absorb the total heat flux, qL, from the block. This choice of heat sink is assumed to model a vertical heat flux from the upper surface of the fluid to the right and left of the floating block.

The principal assumptions of this model are: that d is very small compared to L; that the flow, u, in the " channel " d is laminar, i.e. that the channel Reynolds number is small compared to one; that the flow in the regions to the right and left of the block cause density fluctuations which are small compared to $\rho-\rho_1$; that the thermal diffusion time across the channel, d^2/κ, is small compared to the mass transport time along the channel $L/|u|$. The consistency of the following flow process is to be studied: starting with $L_1 \simeq 0$, the heating qL cause the density of region L_1 to fall to ρ_1; due to the resultant pressure head, the horizontal force on the block, F_1-F gives rise to a block velocity, V, to the left; the resulting channel velocity, u, and heating, qL, are just sufficient so that the fluid emerging into region L_1 has decreased its density from ρ to ρ_1. We assume that the heat capacity, C, the coefficient of thermal expansion, α, and the kinematic viscosity, ν, of the fluid are constants. It would be compatible with this flow model to presume that the viscosity increased with height above the bottom, i.e. with temperature,

so that the flow, u was confined to the bottom region until reaching the right-hand wall. Ascending flow along the right-hand wall then could be thought of as modeling the mid-Atlantic upwelling with a symmetrically disposed second block moving off to the right of Fig. 2.

In order to use the simple Boussinesq description of the flow we will restrict attention to density contrasts, $\rho-\rho_1$, which are small compared to the density ρ. Then, for a steady-state to be maintained

$$F_1-F = \frac{g}{2}[\rho_1(h_1-d)^2-\rho(h-d)^2] = -\nu\rho L u_z(d) \qquad (2.1)$$

where g is the acceleration of gravity, u_z is the vertical gradient of u at the lower boundary of the block, and the right-hand side of Eq. (2.1) is the total viscous stress due to flow in the channel balancing the total horizontal pressure force, (F^1-F), on the vertical sides of the block. For thermal balance of the heat into and out of the channel one must have

$$qL = \frac{Cd}{\alpha}(\bar{u}+V)\Delta\rho \qquad (2.2)$$

where

$$\bar{u} \equiv \frac{1}{d}\int_0^d u(z)\,dz, \quad \Delta\rho \equiv \rho-\rho_1 = \rho\alpha(T_1-T)$$

Hence to determine V, one must compute the laminar Couette–Poiseuille-thermal flow, $u(z)$, in the channel. We seek solutions compatible with a pressure which varies linearly along the channel in the horizontal (x) direction, so that

$$P = g\left[\rho(h-z)\left(1-\frac{x}{L}\right)+\rho_1(h_1-z)\frac{x}{L}\right] \qquad (2.3)$$

We are to find $u(z)$ from the horizontal equation of motion

$$-\nu u_{zz} = -\frac{1}{\rho}P_x \qquad (2.4)$$

subject to the boundary conditions

$$u(0) = 0 \quad \text{and} \quad u(d) = -V \qquad (2.5)$$

The solution of Eqs. (2.3, 4, 5) is

$$u(z) = \frac{gd^2}{2\rho L\nu}\left(\frac{z}{d}\right)\left(1-\frac{z}{d}\right)\left[\frac{\Delta P}{g}-\frac{\Delta\rho}{3}(d+z)\right]-V\left(\frac{z}{d}\right) \tag{2.6}$$

where $(\Delta P/g) = \rho h - \rho_1 h_1$.

Hence, from Eq. (2.6) one finds that

$$\bar{u} = \frac{gd^2}{12\rho L\nu}\left(\frac{\Delta P}{g}-\frac{\Delta\rho d}{2}\right)-\frac{V}{2} \tag{2.7}$$

and

$$u_z(d) = -\frac{gd}{\rho L\nu}\left(\frac{\Delta P}{2g}-\frac{1}{3}\Delta\rho d\right)-\frac{V}{d} \tag{2.8}$$

We note that

$$\rho_1 h_1^2 - \rho h^2 = \rho h^2\left(\frac{(1-\Delta P/\rho g h)^2}{(1-\Delta\rho/\rho)}-1\right) \simeq \rho h^2\left[\frac{\Delta\rho}{\rho}-2\frac{\Delta P}{\rho g h}\right] \tag{2.9}$$

for

$$\Delta\rho/\rho \ll 1 \quad \text{and} \quad \Delta P/\rho g h \ll 1.$$

Therefore, with the use of Eqs. (2.8) and (2.9), the force balance Eq. (2.1) may be written

$$\tfrac{1}{2}(h^2-d^2)\Delta\rho-(h-d)\frac{\Delta P}{g} = \frac{d}{2}\frac{\Delta P}{g}-\frac{d^2}{3}\Delta\rho+\frac{\rho L\nu}{gd}V \tag{2.10}$$

Hence Eqs. (2.2), (2.8) and (2.10) represent three equations for the four unknown $\bar{u}$, V, ΔP, and $\Delta\rho$. A fourth equation relating these variables is found from the conditions for the continuity of mass flow between regions to the right and left of the drifting block. For the left region

$$L_2\frac{\partial\rho h}{\partial t} = \rho(h-d)V-\rho d\bar{u} \tag{2.11}$$

and for the right region

$$L_1\frac{\partial\rho_1 h_1}{\partial t} = -\rho_1(h_1-d)+\rho d\bar{u} \tag{2.12}$$

For a steady solution to Eqs. (2.7), (2.8) and (2.10), both ΔP and $\Delta\rho$ must be independent of time. From Eqs. (2.11, 12) one finds that ΔP is independent of time when

$$\rho d\bar{u} = \left[\rho(h-d)-\left(\frac{\Delta P}{g}-d\Delta\rho\right)\left(1-\frac{L_1}{L_1+L_2}\right)\right]V \simeq \rho(h-d)V \tag{2.13}$$

the right-hand relation holding for small $\Delta\rho$ and ΔP. We will return to the conditions imposed on ρ, ρ_1, h, h_1 by the time independence of $\Delta\rho$ in the following paragraph. Equation (2.13) completes the set of equations needed to determine solutions for $\bar{u}$, V, ΔP, and $\Delta\rho$. Then from Eqs. (2.2), (2.8), (2.10) and (2.13) we find that

$$V^2 = \left(\frac{\alpha g q h^2}{24\rho C\nu}\right)F\left(\frac{d}{h}\right) \tag{2.14}$$

where

$$F\left(\frac{d}{h}\right) = \left(\frac{d}{h}\right)^3\left[1-\frac{d}{h}+\tfrac{1}{6}\left(\frac{d}{h}\right)^2\right]\Big/\left[1-\frac{d}{h}+\tfrac{1}{3}\left(\frac{d}{h}\right)^2\right]$$

One finds also that

$$\Delta\rho = \left(\frac{\alpha g L}{Ch}\right)\frac{1}{V} \tag{2.15}$$

and that

$$\frac{\Delta P}{g} = \left(\frac{12\rho L\nu(h-d/2)}{gd^3}\right)V+\left(\frac{\alpha q L d}{2Ch}\right)\frac{1}{V} \tag{2.16}$$

The steady solutions Eqs. (2.14, 15, 16) are possible when $\Delta\rho$ as well as ΔP are time independent. In addition, Eqs. (2.11, 12) for mass continuity require that when ΔP is constant, then independently

$$\frac{\partial\rho h}{\partial t} = 0, \qquad \frac{\partial\rho_1 h_1}{\partial t} = 0 \tag{2.17}$$

to first order in the small quantities ΔP and $\Delta\rho$. A final relation determining the time dependence of ρ, ρ_1, h, h_1 is the requirement that the total production of heat is balanced by a uniform sink of heat in the fluid. This latter condition, plus the constancy of $\Delta\rho$ and Eq. (2.17) leads to

$$\frac{\partial \ln \rho}{\partial t} = \frac{\partial \ln \rho_1}{\partial t} = -\frac{\partial \ln h}{\partial t} = -\frac{\partial \ln h_1}{\partial t} = \frac{-\alpha q}{C\rho^2 h}\left(\frac{L_1+L_2}{L} + \frac{d}{h}\right)^{-1} \tag{2.18}$$

We conclude that the drifting block moves from the right symmetry plane to the left at a constant speed given by Eq. (2.14), uniformly creating as much new fluid of density ρ_1 as is destroyed by the uniform sink. Upon reaching the left symmetry plane, the block reverses its direction and moves to the right. The turn-around time depends on the magnitude of the (neglected) second-order terms in $\Delta\rho$ and the thermal diffusion velocity in the channel. Hence, $\Delta\rho$ can always be chosen sufficiently small so that the turn-around time is a negligible fraction of the block transit time, $(L_1+L_2)/V$.

The most significant conclusion is that the velocity V Eq. (2.14), depends on the fluid parameters and the heating rate in the same manner as does the final velocity U, Eqs. (1.30, 31, 32) for the drifting line source treated in section 1. The two expressions differ in that Eq. (2.14) contains the geometric factors (h/L) and (d/h), and in that there is no value of heating or depth d for which the motion vanishes.

3. Laboratory Experiments with Drifting Heat Sources

In this section the first results from a continuing study of drifting heat sources is presented. The experimental arrangement simulates the line heat source model of section 1 since that theory provides a description of the entire flow field.

The principal observable with which we were concerned was the velocity of the source as a function of the heating rate, geometric and fluid parameters. We sought also to discover whether an isolated heat source could propagate itself due to its own fluid motion, as is suggested in the results of section 1.

A variety of floats were used, all of which were heated by passing electric current through stainless steel wires. The electricity reached the floats through 0.005 cm diameter copper wires. When hung limply from above these lead wires produced negligible forces on the floats. The two types of sources reported upon here are; first, floating polyethylene strips with wires stretched beneath them and second, wires contained in hollow aluminum oxide tubes floated by styrofoam pontoons at their ends.

Silicone oils of various viscosities were used as the fluid. The tank containing this fluid was 30 cm wide, 40 cm long and 10 cm high. The bottom of the tank was covered with 0.5 cm of mercury in order to approximate the isothermal, slip boundary conditions used in the theory. The fluid was bounded above by air which, although providing the appropriate slip boundary condition, had two disadvantages. The first was that convection into the air did not provide a sufficiently isothermal surface. The second was that surface tension gradients, due to this variation of surface temperature, could be large enough to influence the source velocity. Although an experimental method exists to remove these difficulties, it was found that their effect on the observations could be adequately estimated.

Preliminary experiments with the polyethylene floats made us aware of the importance of any asymmetry in the heat source-float geometry. When a heating wire was positioned even slightly to one side of the center of its supporting flotation strip, invariably they would move in the direction of the less heated side. We concluded that only the very symmetric oxide tube source was suitable to simulate the theoretical line source of section 2. However, some data for an asymmetric source is included in Fig. 4 and will be discussed shortly.

The typical time trajectories of two oxide tube floats, for $R_a = 0$ and for two very different values of R, are shown in Fig. 3. The most striking feature of these observations is the constancy of the velocity of separation for many dimensionless length units after the power is first turned on. The second feature of importance is the gradual reduction in velocity at large separation.

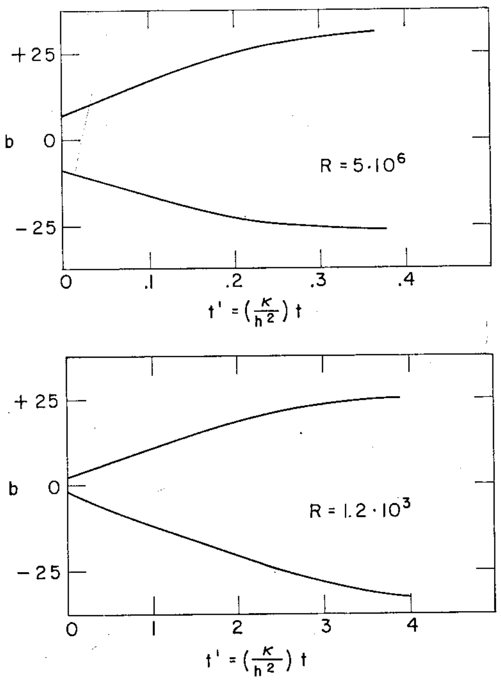

Figure 3. Typical displacement versus time curves for a pair of line heat sources. Note the difference in time scales.

Neither result is in keeping with the theoretical deduction Eq. (1.29). In the theory, the initial velocity of separation should depend linearly on R and drop off as $\exp(-b)$. The final velocity should be constant and depend linearly on the square root of R. We have concluded, tentatively, that: a thermal boundary layering process resulting from higher-order terms in the R expansion is responsible for the initial constant velocity at moderately large b. We conclude, also, that the solution for great separation distance, Eq. (1.30), is not stable for highly symmetric sources, at least not sufficiently stable to overcome the small three-dimensional end effects and float drag. However, the magnitude of the velocity of the source is in keeping with the theory, as is reported in the following paragraph.

A series of experiments were performed to determine the

initial velocity as a function of R. The value of R was changed by varying the depth of 60,000 centistoke oil, the depth varying from 5 cm to 0.25 cm. Only two different heating powers were used, 0.5 watts per cm and 1 watt per cm. In this way it was hoped that spurious forces due to surface tension, end effects and float drag would be the same in all the experiments. The data for these experiments is plotted in Fig. 4 as (+). The solid line in this

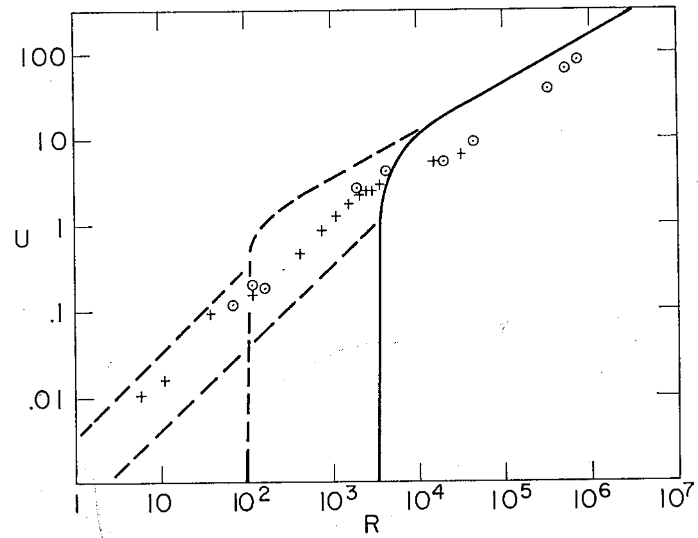

Figure 4. Velocity of line sources versus heating parameter, R. Datum for symmetric source pair is indicated by +. Datum for a single asymmetric source is indicated by ⊙. The solid curve is Eq. (1.32). Dashed curves are discussed in the text.

figure is the theoretical result Eq. (1.32) in which U varies as the square root of R. The lower dashed line represents the maximum value of U versus R from Eq. (1.29). The upper dashed line is an approximate solution similar to Eq. (1.29), but with the upper boundary of the fluid taken to be an insulator rather than isothermal. Evidently, there is some reasonable agreement with theory, which might be improved if float drag and end effects can be reduced.

The circular data points (⊙) in Fig. 2 are for a single float which was purposely made asymmetric. It is seen that its velocity dependence on R is very similar to that of the parting float pairs. Dr. Alan Newell, in conversation, pointed out to us that source asymmetry could easily be incorporated into the analysis of section 1. If the line source in Eq. (1.2) is taken as $[\delta(x-a)+\gamma\delta'(x-a)]$ where $\gamma \leqslant 1$ and δ' is the derivative of the delta function, then the source velocity becomes proportional to γ at large separation distances.

The preceding data was taken with no heating from below, i.e.

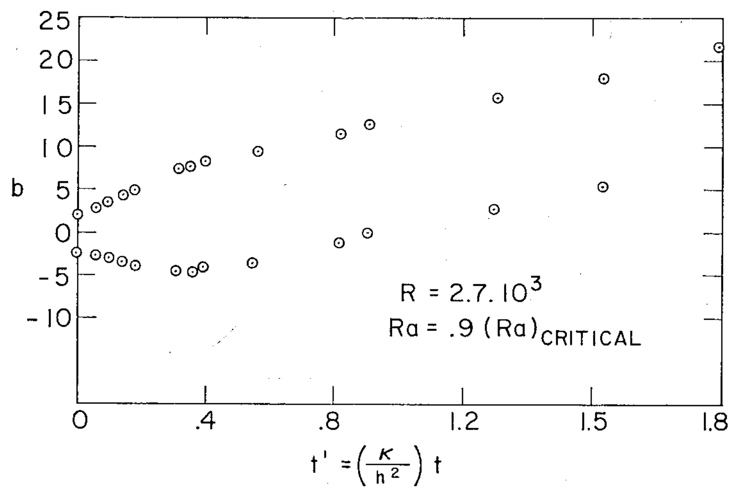

Figure 5. Displacement versus time record for a symmetric line source pair in a fluid heated from below.

for $R_a = 0$. A very few experiments have been made for R_a close to its critical value for free convection. A typical trajectory for $R_a = 0.9(R_a)_c$ is shown in Fig. 5. The fluid, floats and geometry were the same as those of Fig. 4. It is seen that the floats separate until they reach a distance $b = 12.5$, after which they maintain this separation and move off together at a reduced velocity. As one might have anticipated, this spacing is the exact size of the free convection cell which would first occur if the fluid were unstable $[R_a > (R_a)_c]$. It seems likely that the final velocity of the pair of floats is due to a slight difference in their source

strengths. No studies have been made yet in the range $R_a > (R_a)_c$. It will be of considerable interest to discover the area in the R, R_a plane in which the floating sources dominate the convective process.

4. Geophysical Implications

The experiments and the theories of both sections 2 and 3 suggest that source drift velocities proportional to the square root of the heating rate can be expected to occur in a fluid differentially heated by the floating sources. Theory and experiment also suggest that the drift velocity is independent of the thermometric conductivity of a fluid with a large Prandtl number.

A qualitative consequence of the model of section 3 is that the heat flux q emerges from the "ocean" regions, although it is produced in the "continent". We presume, of course, that a similar heat flux emerges from the top of a realistic continent. In applying this model to the earth one must add the horizontally homogeneous heat sources and the appropriate adiabatic lapse rate to the Boussinesq description of the vertical temperature distribution. Hence the model does not require that heat actually flow down, but only that the differential heating produces temperature variations in the horizontal.

To determine the magnitude of drift velocity from Eq. (2.14), we have assumed that the differential heating rate between continent and ocean is approximately $q = 10^{-6}$ cal/sec cm. We have chosen $h = 6.10^7$ cm, as this is the largest depth at which there is evidence for significant motion. The source depth is taken to be $(h-d) = 3.10^6$ cm. However $F(d/h)$ of Eq. (2.14) is quite insensitive to this choice. The principal uncertainty is the value of the kinematic viscosity. Pekeris (1935), and Turcotte and Oxburgh (1969a, b), have used Haskell's (1935) value of $\nu = 3.10^{21}$ poises, estimated from the Fennoscandia post-glacial uplift. The parameter group $(\alpha g/\rho c)$ is taken to be $2.5 \cdot 10^{-2}$ cm^4/cal sec^2 with confidence that the uncertainty in this value is small compared to the uncertainty for the values of ν and h. With these estimates used in Eq. (2.14) we find that

$$V_{\text{continent}} \simeq 3.10^{-8} \text{ cm/sec} \simeq 1 \text{ cm/yr}$$

As a consequence, the density contrast $\Delta\rho/\rho$ across a continent of $L = 5.10^8$ cm is less than 10^{-2} from Eq. (2.15). Also, one finds from Eq. (2.16) that the difference in pressure head across the continent is approximately 3.10^5 cm. A discussion of the strength of the crustal material and whether the estimated forces are sufficient to account for the observed breaking, folding, and flowing will not be attempted here.

Acknowledgements

The authors are indebted to several geophysicists for discussion and advice. We are particularly grateful to G. Oertel for discussions in the Spring of 1968 which led to a first crude experiment with drifting heat sources. We are indebted to D. Griggs and L. Knopoff for their continuing interest in the details of this study. Finally we wish to thank L. Slichter for his encouragements and early observation that we sought to study " the first nuclear-powered vessels " in the world ocean.

This work was partially supported by grants from the Office of Naval Research and the National Science Foundation.

REFERENCES

Haskell, N. A., " The motion of a viscous fluid under a surface load," *Physics* **6**, 265 (1935).

Isacks, B., Oliver, J. and Sykes, L. R., " Seismology and the New Global Tectonics," *J. Geophys. Res.* **73**, 5855–5899 (1968).

Pekeris, C. L., " Thermal convection in the interior of the earth," *Monthly Notices Roy. Astron. Soc., Geophys. Suppl.* **3**, 343 (1935).

Turcotte, D. L. and Oxburgh, E. R., " Convection in a mantle with variable physical properties," *J. Geophys. Res.* **74**, 1458 (1969).

Turcotte, D. L. and Oxburgh, E. R., " Continental Drift," *Physics Today* (April 1969).

Geophysical Fluid Dynamics. 1970. Vol. 1 pp. 143–160

Printed in Great Britain

A Hydrodynamic Curiosity: the Salt Oscillator

SEELYE MARTIN

Department of Oceanography
University of Washington
Seattle

Abstract—If a vertically oriented hypodermic syringe with the plunger removed is filled with salt water and partially submerged in a beaker of fresh water, then under the proper conditions, the system develops finite amplitude oscillations. These oscillations appear as a downward jet of salt water, followed by an upward jet of fresh water, and so on for many cycles. The geometry of the syringe determines the period of the oscillations: a long, small diameter needle yields a slow, viscous flow; a short, large diameter needle yields fast inviscid pumping. Theoretically, a time-dependent Hagen–Poiseuille pipe flow model describes the oscillations; furthermore, the oscillations can be divided into two modes, depending on whether viscous or non-linear damping predominates. When viscous damping predominates, the geometry of the syringe determines the period of the oscillations, which are independent of the density difference $\Delta\rho$ except as the viscosity varies with density. When non-linear damping predominates, the period is proportional to $(\Delta\rho)^{1/2}$. Experiments confirm the existence of both modes.

1. Introduction

A variety of straight tubes whose cross-sectional area varies with lengths (such as funnels, hypodermic syringes, pipettes, and tin cans with pin holes in the bottom) when filled with salt water and partially submerged in a beaker of fresh water will exhibit finite amplitude oscillations. These oscillations appear as a downward jet of salt water, followed by an upward jet of fresh water, and so on for many cycles (Fig. 1). For example, a tin can of radius 3.3 cm with a pin hole in the bottom, which was initially filled to a depth of 8 cm with a saturated solution of sodium chloride, produced oscillations with a period of 40 sec and ran for four days. A hypodermic syringe with a volume of 10 cm^3, in an experiment

GEOPHYSICAL FLUID DYNAMICS

A Journal of the Mechanics and Energetics of Atmospheres and Ocea

Volume I Numbers I and 2 April 1970 Pages I - 272

GORDON AND BREACH SCIENCE PUBLISHERS
New York · London · Paris